The Journal of Experimental Biology 207, 633-644
Published by The Company of Biologists 2004
doi:10.1242/jeb.00784

Modular organization of the silkmoth antennal lobe macroglomerular complex revealed by voltage-sensitive dye imaging

Hiroyuki Ai* and Ryohei Kanzaki†

Institute of Biological Sciences, University of Tsukuba, Tsukuba, Ibaraki 305-8572, Japan

*Present address: Division of Biology, Department of Earth System and Sciences, Fukuoka University, Fukuoka 814-0180, Japan
†Author for correspondence (e-mail: kanzaki@biol.tsukuba.ac.jp)

Accepted 10 November 2003

Summary

We succeeded in clarifying the functional synaptic organization of the macroglomerular complex (MGC) of the male silkmoth *Bombyx mori* by optical recording with a voltage-sensitive dye. Sensory neurons in the antennae send their axons down either the medial nerve (MN) or lateral nerve (LN), depending on whether they are located on the medial or lateral flagella. Pheromone-sensitive fibers in the MN are biased towards the medial MGC, and those in the LN are biased towards the lateral MGC in the antennal lobe. In our optical recording experiments, the postsynaptic activities in the MGC were characterized by pharmacological analysis. Postsynaptic activities in the MGC were separated from sensory activities under Ca^{2+}-free conditions, and subsequently the inhibitory postsynaptic activities were separated by applying bicuculline. We found that the inhibitory postsynaptic responses always preceded the postsynaptic responses separated under Ca^{2+}-free conditions. Moreover, the excitatory postsynaptic activities were calculated by subtracting the inhibitory potentials from the posysynaptic activities separated under Ca^{2+}-free conditions. When the MN was stimulated, the amplitudes of the excitatory postsynaptic activities in the central toroid, the medial toroid and the medial cumulus were selectively higher than those in the other areas. By contrast, when the LN was stimulated, excitatory postsynaptic activities were evoked in areas in both the lateral toroid and the lateral cumulus. The inhibitory postsynaptic activities were equally distributed throughout the whole MGC. These data suggest that there is a modular organization to the MGC such that information from the two main branches of the antenna is segregated to different sub-regions of the MGC glomeruli.

Key words: insect, *Bombyx mori*, optical recording, postsynaptic response, GABA, topology, brain.

Introduction

Topographic projections from the sensory epithelium into the olfactory bulb in vertebrates (Jastreboff et al., 1984; Pederson et al., 1986; Shepherd, 1993; Schoenfeld et al., 1994) and from the antenna into the antennal lobe (AL) in invertebrates (Koontz and Schneider, 1987; Christensen et al., 1994) have been demonstrated. The AL is the primary olfactory center in the insect brain. In the silkmoth *Bombyx mori*, the macroglomerular complex (MGC) in the AL is a male-specific structure and the area where the terminals of sensory afferents make contact with the dendritic processes of a subset of pheromone-processing interneurons (Kanzaki and Shibuya, 1986; Kanzaki et al., 2003). In *B. mori* and the tobacco hornworm *Manduca sexta*, two large glomeruli, the toroid and cumulus, are easily distinguishable in the MGC (Hansson et al., 1991; Kanzaki et al., 2003). An immunocytochemical study examining acetylcholinesterase levels in these two glomeruli showed uniformly fibrous acetylcholinesterase staining that was noticeably more dense in the toroid in *M. sexta* (Homberg et al., 1995). It has been suggested that these differences could reflect a heterogeneous distribution of synapses in different parts of the MGC (Homberg et al., 1995).

To date, little has been reported about the processing of the information of the topology of the antenna. In the American cockroach *Periplaneta americana*, the projection neurons can be assigned to two subgroups on the basis of their receptive fields from the antenna. An identified neuron with local receptive fields has profusely branching dendrites in the lateral region of the macroglomerulus (MG). Another identified neuron with global receptive fields has dendrites uniformly distributed throughout the MG. However, it is not clear whether there is spatial partitioning of the pheromone response in the macroglomerular projection neurons according to which region of the antenna is stimulated (Hosl, 1990). In *M. sexta*, the arborizations of the macroglomerular complex projection neurons (MGC-PNs) with different receptive fields are similar in terms of extent, indicating there is no spatial partitioning of the pheromone response in the MGC according to which region

of the antenna is stimulated (Heinbockel and Hildebrand, 1998). To investigate whether there is a spatial partitioning in the MGC, it is necessary to compare the postsynaptic activities in the MGC sub-regions. We succeeded in separating postsynaptic activities from presynaptic activities in the AL pharmacologically by using optical recording techniques (Okada et al., 1996; Ai and Inouchi, 1996; Ai et al., 1998). Moreover, it has become possible to separate the postsynaptic activities from the presynaptic activities in the MGC sub-regions using this technique. In the present study, the postsynaptic activities were compared between the MGC sub-regions.

In *B. mori*, the antennal nerve (AN) bifurcates into the medial nerve (MN) and the lateral nerve (LN; Koontz and Schneider, 1987). In the present study, these two distinct pathways from the antennae to the MGC were characterized by optical recording in order to understand the functional synaptic organization of topological information through the sensory fibers of the AN to the MGC.

Materials and methods

Pupae of silkworm moths (*Bombyx mori* L.; Lepidoptera: Bombycidae) were purchased from Kyoya Industries Co., Kyoto, Japan. Adult male silkworm moths were used within 2–4 days of eclosion.

Histology

To investigate the source of the MN and the LN in the antenna, the sensory fibers of either the MN or the LN were retrogradely stained with 0.1 mol l^{-1} cobalt-lysine for 24 h at 4°C. Pharate adults before melanization were used because the stained fibers were hard to differentiate from the outside of the cuticle of the antenna in melanized adults. The antenna was rinsed in saline, developed in hydrogen sulfide gas and fixed in 4% paraformaldehyde for 24 h at 4°C. The brain was subsequently intensified with silver (Bacon and Altman, 1977), dehydrated and cleared by methylsalicylate. To clarify projection areas of sensory axons through the MN and LN, the brains were dissected from the head and then the cut end of either the MN or the LN was immersed in 1% tetramethylrhodamine–dextran solution (Molecular Probes, Eugene, OR, USA). The bundles were exposed to this solution for 24 h at 4°C. The brains were prefixed in 4% paraformaldehyde in 0.2 mol l^{-1} phosphate buffer (pH 7.4) for 2 min and immersed in 0.1% Lucifer yellow solution (Sigma, St Louis, MO, USA) for 4 h at room temperature (Kanzaki et al., 2003). The brains were then fixed in 4% paraformaldehyde for 1 h at room temperature and dehydrated with an ethanol series and cleared in methylsalicylate. Each stained brain was imaged frontally using a laser-scanning microscope (LSM-510; Carl Zeiss, Jena, Germany) with a plan apochromat ×10, ×20 or ×40 objective. Serial optical slices were acquired at 4.0 μm intervals for the ×10 objective, 1.5 μm intervals for the ×20 objective and 1.1 μm intervals for the ×40 objective.

3-D reconstruction of the AL

In order to acquire 3-D reconstruction images of the AL, brains were immersed in 0.1% LY solution for 4 h at room temperature, fixed in 4% paraformaldehyde for 1 h at room temperature, dehydrated with an ethanol series and cleared in methylsalicylate. The brains were viewed with a laser-scanning confocal microscope. Serial optical sections through the AL were acquired at 1.5 μm intervals for the ×20 objective. These images were read into image-processing software (Amira; TGS, Berlin, Germany) to make a 3-D image of the AL.

Optical recording

Optical recording methods employed in this study were essentially identical to those described by Ai et al. (1998). After cooling (4°C, ~30 min) to achieve anesthesia, the animals were initially fixed on an experimental chamber. The head capsule was opened above the brain and most of the muscles in the head were removed. The brain was desheathed using fine forceps, removed from the head capsule and stained with a voltage-sensitive dye (RH414; Molecular Probes; 2–3 mg ml^{-1}) dissolved in physiological saline at room temperature for 5–10 min. Subsequently, excess dye was washed off with physiological saline. In optical recording experiments, the brains were fixed anterior side down on the inverted microscope (Axiovert S100; Carl Zeiss). The brains were mounted on a coverslip (24 mm×32 mm) and held down gently with a strip of coverslip on the posterior side of the brain to prevent movement during perfusion. The aperture between the two coverslips was held at 400 μm by inserting coverslips. The contralateral antennal nerve was also fixed by insertion into a slit of the glass tips (200 μm in width) glued on the coverslips. The recording plane was always focused 50 μm from the surface of the AL because most of the afferent fibers spread around the surface of the AL and enter the glomeruli at this depth. The camera unit of the optical imaging system (Fuji HR Deltaron 1700; Fujifilm Microdevice Co., Tokyo, Japan) is a MOS-type image sensor and has a resolution of 128×128 photopixels. Each photopixel corresponds to a tissue area of 7.16 μm×7.16 μm or 3.58 μm×3.58 μm, depending on whether a 10× (NA, 0.45) or 20× (NA, 0.75) objective is used. The whole array corresponded to an area of 916 μm×916 μm (10×) or 458 μm×458 μm (20×). The excitation filter used in the optical system passed light lengths of 535±25 nm. A dichroic mirror was placed in the light path of a metal halide lamp that was also the emission path as an emission filter (>615nm; KMH-250, BMH-250; Kiyohara Optical Laboratory, Tokyo, Japan).

Data analysis

In our optical recording experiments, a background fluorescence image (F) was acquired, then fluorescence images were acquired every 0.6 ms before, during and after the electrical stimulation (F_x). All these raw data were processed through the following programs. First, each fluorescence change per frame during data acquisition was calculated by subtracting F from each F_x (ΔF). These data were processed

by a '$\Delta F/F$' program to calculate the fractional change of fluorescence divided by the background fluorescence ($\Delta F/F$), then processed by a 'bleaching' program to compensate for photobleaching. Finally, the data were processed by a 'filter' program to separate neural signals from noise. In this study, the signals were cut off above 246 Hz (F_c).

Stimulation

To apply electrical stimulus pulses, both the MN and LN were cut, and the proximal cut stump was held in a glass capillary suction electrode. To prevent leakage of the stimulus pulses to the other nerve, both nerves were isolated by a Vaseline wall at the proximal region of each nerve and were then differentially stimulated. Eight responses to electrical stimulation of the MN or the LN (intensity, ~50 μA; duration, 0.5 ms; 0.2 Hz) were averaged in each recording session. In each preliminary experiment, the intensity of the electrical stimulation of the MN and the LN was fixed to the value that induced the maximal response.

Pharmacological experiments

In our study, we sought to compare the postsynaptic responses blocked under Ca^{2+}-free conditions with the GABAergic responses blocked by a GABA antagonist (bicuculline) for each AL preparation. First, the optical response evoked by electrical stimulation to the MN or the LN was acquired under normal Ringer saline as a control (control for Ca^{2+}-free experiments). Next, the optical responses were acquired after perfusing with Ca^{2+}-free saline for 5–10 min. Then, the optical response was acquired after washing with normal Ringer saline for >10 min (control for bicuculline experiments). Next, the optical response was acquired after perfusing with bicuculline solution for 5–10 min. Finally, the optical response was acquired after washing with normal Ringer saline for >10 min. In our optical recording protocol, the intensity of the signal often slightly decreased with time; however, when the optical response was compared between the postsynaptic response and the GABAergic response, the optical responses were normalized with the peak amplitude of the signal. Ca^{2+}-free saline was adjusted to maintain osmotic pressure by adding 8 mmol l^{-1} $MgCl_2$. (+)-Bicuculline (Sigma) was dissolved in physiological saline within a range of 10^{-7}–10^{-4} mol l^{-1}. Solutions were applied by polyethylene tubes connected to a syringe.

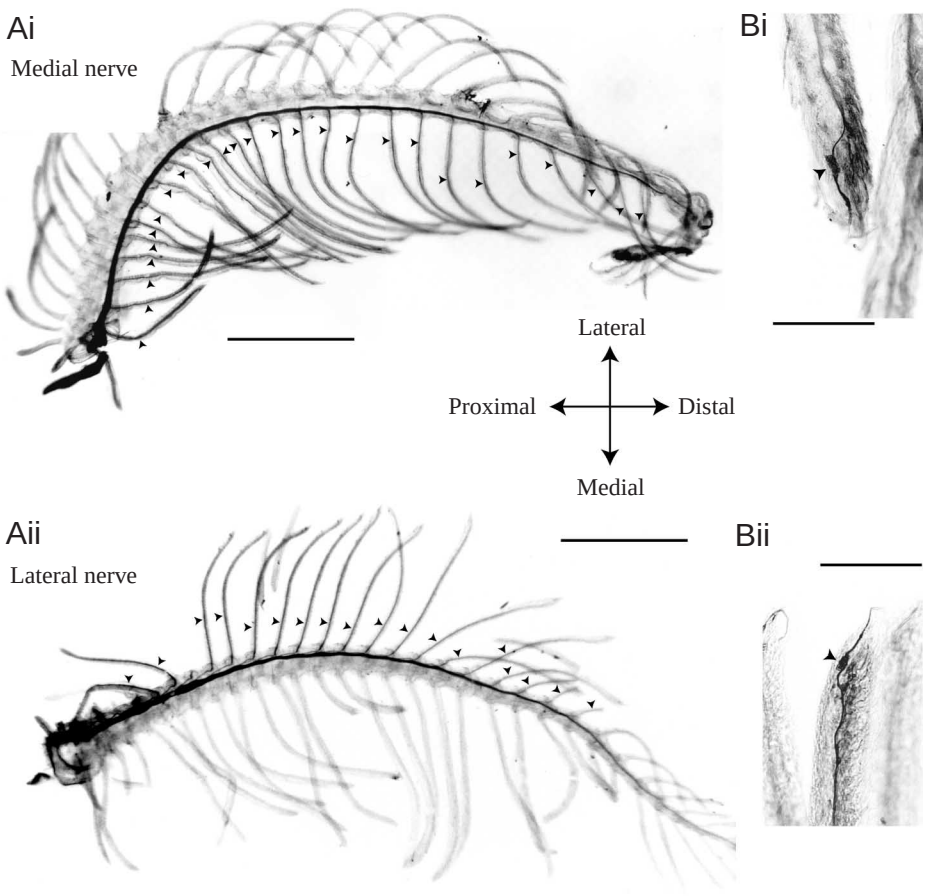

Fig. 1. Sensory fibers stained by back-filling with cobalt-lysine from the cut end of the medial nerve (MN) and the lateral nerve (LN). (A) Axons running in the MN have their source in the medial flagella (arrowheads in i), and axons running in the LN have their source in the lateral flagella (arrowheads in ii). (B) Typical bipolar cells were stained on the surface of the medial flagella (arrowhead in i) and the lateral flagella (arrowhead in ii). Scale bar, 1 mm (A), 100 μm (B).

Results

Relationship between two flagella and the two antennal nerves

The antennal flagella are positioned bilaterally along the antennae as the medial flagella and the lateral flagella (Fig. 1). The AN anatomically bifurcates into the MN and the LN in the second segment of the antenna. To clarify the source of the axons of the MN and the LN in the antenna, the cut end of each nerve was retrogradely stained with cobalt-lysine. In all preparations, axons projecting to the MN were stained in the medial flagella, and axons projecting to the LN were stained in the lateral flagella (Fig. 1A; N=21). Typical bipolar cells were stained on the surface of the antennae of both preparations (Fig. 1B). These results demonstrate that the MN is a bundle of sensory fibers running from the medial flagella, and the LN is a bundle of sensory fibers running from the lateral flagella.

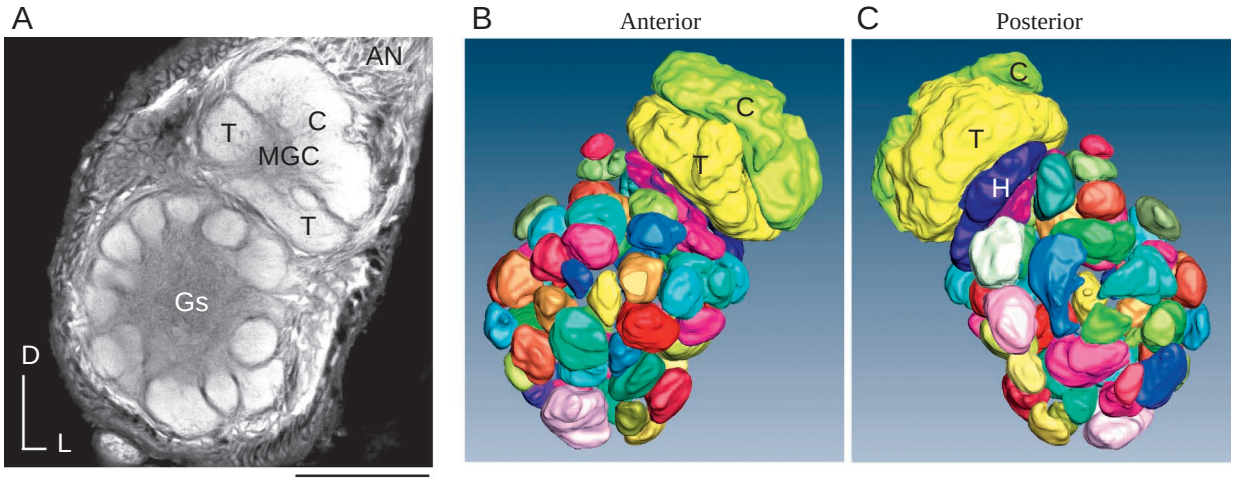

Fig. 2. Antennal lobe (AL) of the silkmoth. (A) Confocal image of the AL. In this focal plane, two macroglomerular complex (MGC) compartments – cumulus and toroid – and 12 ordinary glomeruli are visible in the AL. AN, antennal nerve; C, cumulus; Gs, ordinary glomeruli; T, toroid; D, dorsal; L, lateral. Scale bar, 100 μm. (B,C) 3-D reconstruction images of the AL. These images are from two different directions (anterior and posterior). In the anterior image, the toroid and the cumulus are visible. However, the horseshoe (H) is not visible because this compartment resides near the posterior surface. With our optical recording technique, the anterior side of the AL is always oriented toward the MOS-type image sensors.

Projections of axons from the two antennal nerves to the antennal lobe

The AL contains 58±1 ordinary glomeruli (Gs; diameter 30–50 μm) and the MGC (150–200 μm), which is composed of three compartments: the cumulus, the toroid and the horseshoe (Fig. 2; Ai et al., 1998; Kanzaki et al., 2003). By forward-filling with tetramethylrhodamine–dextran solution from the proximal cut end of the MN (Fig. 3A) or the LN (Fig. 4A), the projection patterns of the axons from the two ANs to the AL were revealed. Both the axons of the MN and those of the LN separately projected towards the AL (Figs 3A, 4A). When the axons of the MN or the LN were filled from the cut end of the AN, a similar pattern of staining was revealed (N=6). The axons of the stained sensory neurons terminated with varicosities (data not shown). The stained axons were 0.5–1 μm in diameter, and their varicosities swelled to 2 μm. It was found that there is a topological bias along the medial–lateral axis in the MGC but not in the ordinary glomeruli (data not shown). The density of the sensory fibers in the MGC is always denser than those in the ordinary glomeruli (Figs 3B, 4B). Sensory fibers in the MN are biased towards the medial MGC; the medial toroid and the medial cumulus were stained more strongly than the lateral toroid and lateral cumulus (Fig. 3B). In the anterior MGC, the bias of the sensory fibers in the MGC was clear (Fig. 3D,E); however, in the posterior MGC, the sensory fibers projected homologously in both the toroid and the cumulus (Fig. 3F). On the other hand, sensory fibers in the LN are biased towards the lateral MGC (N=6); the lateral toroid and the lateral cumulus were stained more strongly than the medial toroid and medial cumulus, respectively (Fig. 4B). In depth of the AL, the bias of the sensory fibers in the MGC was clear (Fig. 4D–F). Thick sensory fibers, probably not olfactory fibers, run through the posterior AL to the antennal mechanosensory and motor center (AMMC), otherwise known as the posterior antennal center (PAC; Figs 3C, 4C).

Optical recording

In this study, we attempted to clarify the spatial partitioning in the MGC related to the topography of the antenna by using optical recording with a voltage-sensitive dye. We used electrical stimulation of the AN and analyzed the optical signals in the MGC, which has been clearly demonstrated to be the sex pheromone processing center in the AL (Kanzaki et al., 2003). Similar spatio-temporal response patterns in the MGC were evoked by electrical stimulation of the MN or the LN in repetitive sessions. In Fig. 5, the pattern was initially depolarization of the AN (3.6–7.2 ms after the onset of the stimulation) and, subsequently, a depolarization of the MGC (4.8–9.6 ms). At 7.2 ms after stimulation of the MN, the depolarization was distributed throughout the MGC, and the area strongly (>0.4% of the background fluorescence) responding to stimulation of the MN was restricted to the medial half of the MGC (Fig. 5B, upper panels). On the other hand, the area strongly (>0.4% of the background fluorescence) responding to stimulation of the LN was restricted to the lateral half of the MGC (Fig. 5B, lower panels). In our preparations, responses in the Gs were also observed but did not have sufficient amplitude for analysis (<0.1% of the background fluorescence). Fig. 5C shows the time courses of the optical signals recorded in the areas that had a response greater than 0.3% ($-\Delta F/F$) at 7.2 ms from the stimuli, evoked by stimulation of the MN or the LN. The response, evoked in the MGC, had a peak at 7.2 ms after the stimulus onset. This time delay varied with each preparation because it depended upon the distance from the stimulation site to the recording region. The negative deflection, as shown in

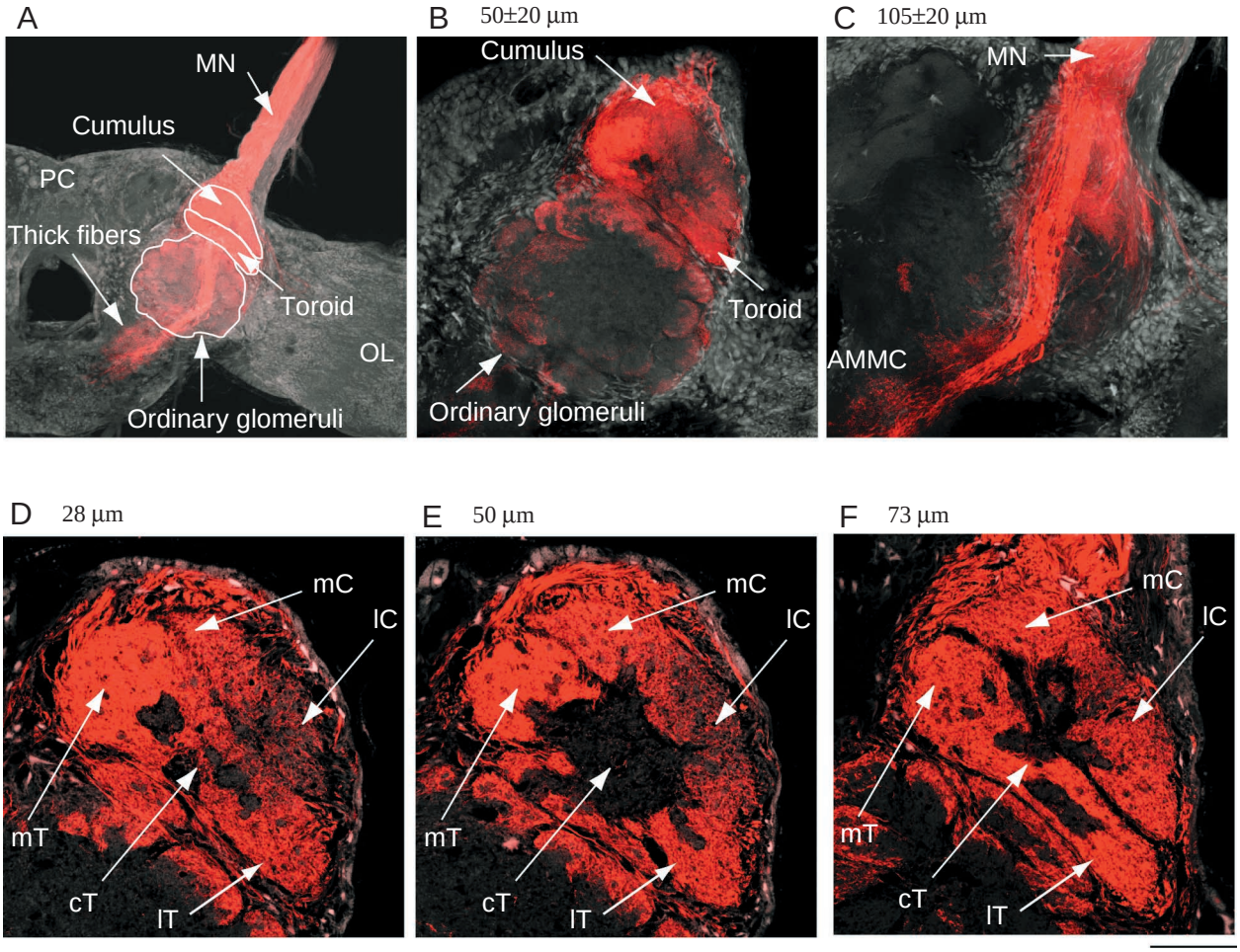

Fig. 3. Projection pattern of the sensory fibers in the medial nerve (MN). (A) The axons were stained by forward-filling from the cut end of the MN with tetramethylrhodamine–dextran. The preparation was counterstained with Lucifer Yellow to visualize the boundary of the tissue. Serial confocal optical slices were acquired and projected to a frontal plane. In the image, the tetramethylrhodamine–dextran-stained fibers were superimposed on the counterstained image of the brain. Axons originating from the MN run through the medial half of the antennal nerve (AN) and project into the antennal lobe (AL). (B) Projected AL image of optical sections at 50±20 μm in depth. The image is of the same preparation as that in A, with a high magnification. The macroglomerular complex (MGC) was always stained more densely than the ordinary glomeruli. The axons projecting to the MGC are biased towards the medial MGC; however, those projecting to the ordinary glomeruli distribute homologously to each ordinary glomerulus. (C) The projected image of the thick axons projecting to the antennal mechanosensory and motor center (AMMC; 105±20 μm in depth). Most of the thin axons running from the MN project to the AL anteriorly, and most of the thick axons project to the AMMC, passing through the posterior AL. (D–F) Confocal images of an anterior plane (D; 28 μm in depth), a medial plane (E; 50 μm in depth) and a posterior plane (F; 73 μm in depth) of the MGC. The MGC is composed of two compartments: toroid, which is a donut-shaped structure, and cumulus, which is a disk-shaped structure situated more proximally to the AN input. In both the anterior and the medial planes, the stained axons are biased towards the medial MGC: medial toroid and medial cumulus. In the posterior plane, the stained axons are distributed homologously. OL, optic lobe; cT, central toroid; mT, medial toroid; lT, lateral toroid; mC, medial cumulus; lC, lateral cumulus. Scale bar, 200 μm (A), 100 μm (B,C), 50 μm (D–F).

Fig. 5C, often appeared when the electrode for the electrical stimulation was placed close to the AL (data not shown). In the following pharmacological experiments, the electrodes were placed at a distance from the AL so that the optical signal didn't include the negative deflection.

Pharmacological analysis

Effects of Ca^{2+}-free saline

As clearly observed in the time course of the optical signals in the MGC elicited by stimulation of the MN or the LN, the responses had another slow component (arrowheads in Fig. 5C) after the first peak of depolarization. When the MN or the LN was stimulated, the slow component had a peak (~5.0 ms) after the first peak (N=8). To investigate the source of the slow component, pharmacological experiments were applied to the AL with optical recording. In *M. sexta*, the axons of antennal olfactory receptor neurons make chemical synapses with dendrites of AL neurons (Tolbert and Hildebrand, 1981). Since chemical synaptic transmission is blocked under Ca^{2+}-free conditions, electrical stimulation of the AN successfully

excites only primary neurons. Therefore, by subtracting the optical responses under Ca^{2+}-free saline conditions from those under normal saline conditions we can separate possible postsynaptic activities (Ai et al., 1998). When the MN was electrically stimulated, the optical responses were measured in the whole MGC; in three regions of the toroid (medial, central and lateral toroid) and two regions of the cumulus (medial and lateral cumulus) (Fig. 6A). These five regions have the characteristic features of the 3-D structure of the MGC as follows: (1) medial toroid (mT) is the densely stained region observed by forward-filling of the tetramethylrhodamine–dextran solution from the MN, through the anterior to posterior plane of the MGC (Fig. 3D–F); (2) lateral toroid (lT) is the densely stained region observed by forward-filling of the tetramethylrhodamine–dextran solution from the LN, through the anterior to posterior plane of the MGC (Fig. 4D–F); (3) central toroid (cT) is a region where there is a core structure composed of axons of AL interneurons (Figs 3E, 4E) and, on both the anterior (Figs 3D and 4D) and the posterior planes (Figs 3F, 4F), there are some projecting terminals from both the MN and the LN; (4) medial cumulus (mC) is the medial half of the cumulus (Figs 3D–F, 4D–F); (5) lateral cumulus (lC) is the lateral half of the cumulus (Figs 3D–F, 4D–F). The AL in the real image of optical recording was superimposed on the typical 3-D confocal image of the AL (Fig. 2B, anterior) by fitting the outline of the AL, and then the boundary between the toroid and cumulus were determined in the optical recording images. The toroid was then divided equally into three sections: mT, cT and lT. When the MN was stimulated, the peak amplitudes of the optical responses in each mT, cT and mC were always larger than that in each lT and lC. In each MGC sub-region, the slow component of responses was blocked under Ca^{2+}-free conditions (arrowheads in Fig. 6A). These results indicate that the slow component was caused by postsynaptic activities in the MGC. In the toroid, the peak amplitude of the slow component of the optical signals in both

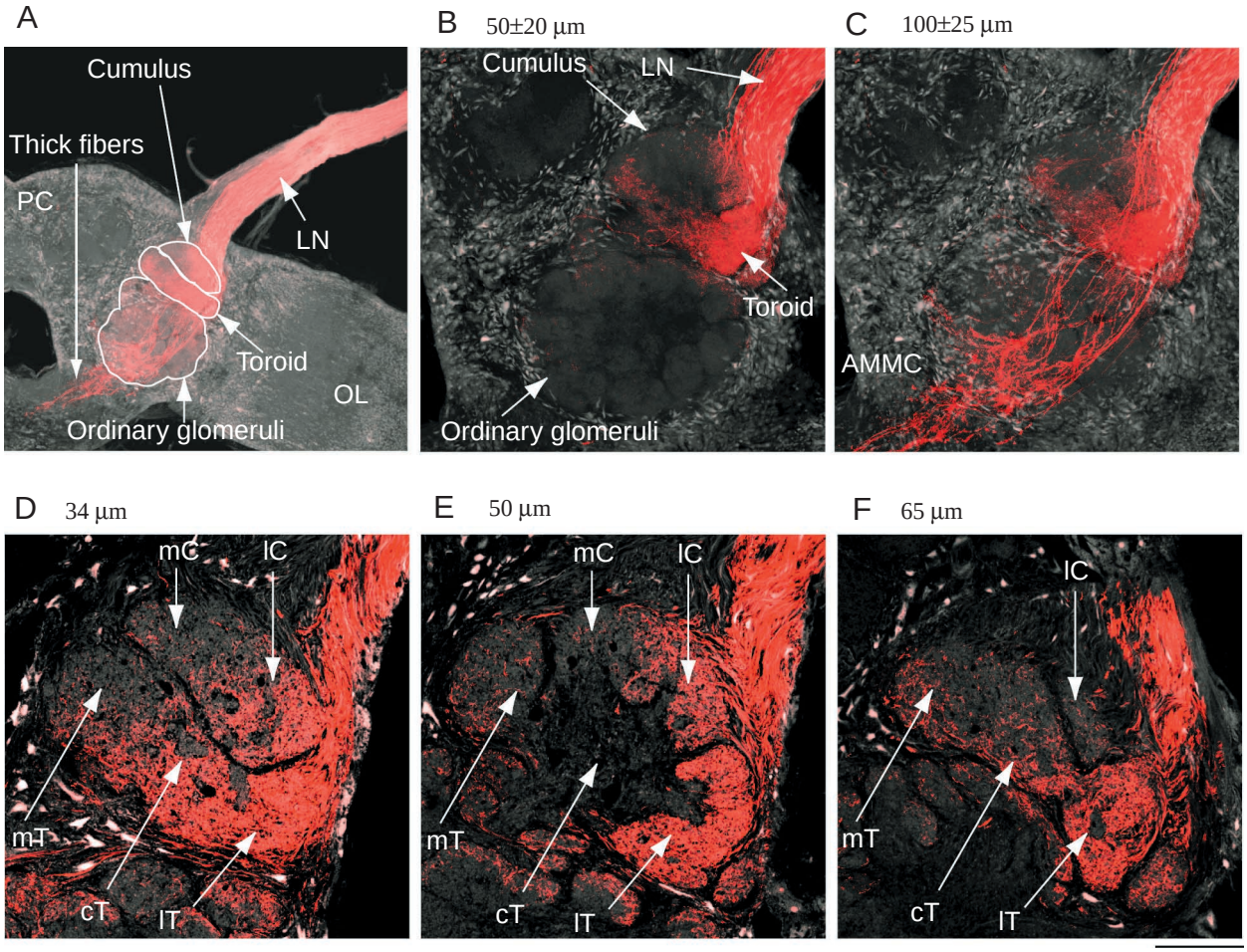

Fig. 4. Projection pattern of the sensory fibers in the lateral nerve (LN). (A) Axons originating from the LN run through the lateral half of the antennal nerve (AN) and project to the antennal lobe (AL). (B) Projected AL image of optical sections at 50±20 μm in depth. The image is of the same preparation as that in A, with a high magnification. The axons projecting to the macroglomerular complex (MGC) are biased towards the lateral MGC. (C) The projected image of the thick axons projecting to the antennal mechanosensory and motor center (AMMC; 100±25 μm in depth). (D–F) Confocal images of an anterior plane (D; 34 μm in depth), a medial plane (E; 50 μm in depth) and a posterior plane (F; 65 μm in depth) of the MGC. In all optical planes, the stained axons are biased towards the lateral MGC; lT and lC. For abbreviations, see Fig. 3. Scale bar, 200 μm (A), 100 μm (B,C), 50 μm (D–F).

the mT and cT evoked by electrical stimulation of the MN was significantly larger than that of the lT (mT>lT, $P<0.05$; cT>lT, $P<0.05$; one-way repeated-measures ANOVA; Fig. 7A). In the cumulus, the peak amplitude of the slow component in the optical signals in the mC evoked by electrical stimulation of the MN was also significantly larger than that of the lC (mC>lC, $P<0.05$; one-way repeated-measures ANOVA; Fig. 7A).

When the LN was electrically stimulated, optical responses were evoked in the lT and lC (Fig. 8A). In the lT and the lC, the slow components were isolated under Ca^{2+}-free conditions (arrowheads on red lines in Fig. 8A). In the other MGC sub-regions, the slow component was hardly observed (red lines in Fig. 8A).

With both MN stimulation and LN stimulation, the slow components gradually increased from 1.5±0.5 ms after the first peak, then rapidly decreased after 3.7±0.7 ms and disappeared at 24.4±2.5 ms (mean ± S.E.M., N=7). After washing with normal saline (5 min), the time course of the falling phase recovered to that under normal saline.

Effects of bicuculline

We have demonstrated that many GABA-like immunoreactive neurons exist in the AL of male *B. mori* (Yokokawa and Kanzaki, 1997). In order to separate possible GABAergic secondary responses, optical recordings were made under GABA blocker conditions. When the MN was stimulated, bicuculline had no effect on the first peak of the optical response but increased the slow component of the optical response (arrowheads in all MGC sub-regions in Fig. 6B). When the LN was stimulated, bicuculline had no effect on the rising phase of the optical response but increased the intensity of the falling phase of the optical response (arrowheads in MGC sub-regions except mT in Fig. 8B). The differences in the time courses of the response amplitudes were caused by blocking the secondary GABAergic inhibitory potentials of AL interneurons. Therefore, the possible time courses of the GABAergic inhibitory potentials were calculated by subtracting the responses under bicuculline conditions from those under normal conditions (Ai et al., 1998). The GABAergic inhibitory potentials gradually increased from 0.2±0.2 ms and reached a peak at 2.8±0.5 ms, then gradually decreased (mean ± S.E.M., N=7). The delay time of the GABAergic inhibitory potentials from the first peak (0.2±0.2 ms) was shorter than the delay time of the postsynaptic activities blocked by Ca^{2+}-free saline

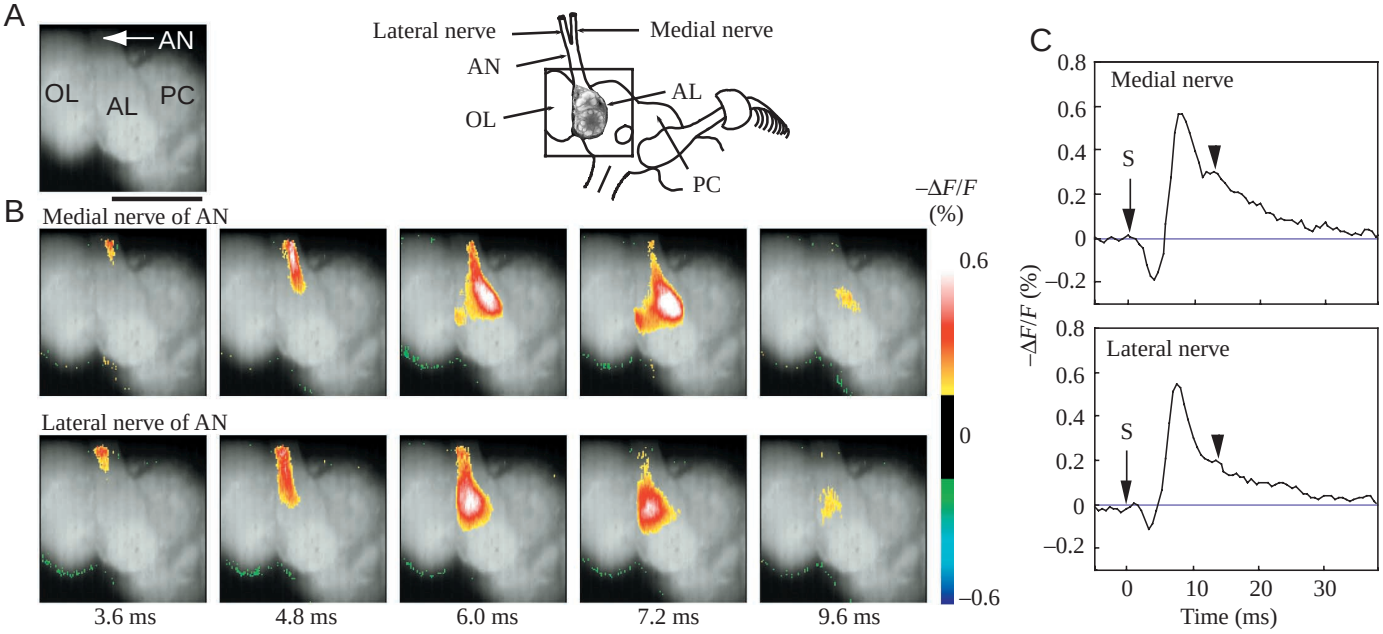

Fig. 5. Optical responses in the antennal lobe (AL) elicited by electrical stimulation of the medial nerve (MN) and the lateral nerve (LN). (A) Real image of the moth brain (boxed area of inset). The boxed area in the schematic drawing corresponds to the MOS-type image sensor used by optical recording. Scale bar, 500 µm. OL, optic lobe; PC, protocerebrum. (B) Optical responses in the AL. All optical images were superimposed on the bright real image of the AL. Consistent response patterns in the macroglomerular complex (MGC) were evoked by the electrical stimulation of the medial nerve (MN) or the lateral nerve (LN). The pattern was initially a depolarization of the antennal nerve (AN; 3.6–7.2 ms after the onset of the stimulation) and, subsequently, a depolarization of the MGC (4.8–9.6 ms). At 7.2 ms from the stimulus of the MN, the area strongly (>0.4% of the background fluorescence) responding to stimulation of the MN was restricted to the medial half of the MGC. By contrast, the area strongly (>0.4% of the background fluorescence) responding to stimulation of the LN was restricted to the lateral half of the MGC. (C) Time course of the optical signals in the AL evoked by stimulation of the MN (upper panel) and the LN (lower panel). The optical signal was calculated by averaging signals recorded in areas that had a response of >0.3% ($-\Delta F/F$) at 7.2 ms from the stimulus onset and filtered at 246 Hz (F_c). The response, evoked in the MGC, had a peak at 7.2 ms after the stimulus onset. The response had another slow component (arrowheads) after the first peak of the depolarization. The annodal break was visible just after the stimuli (S).

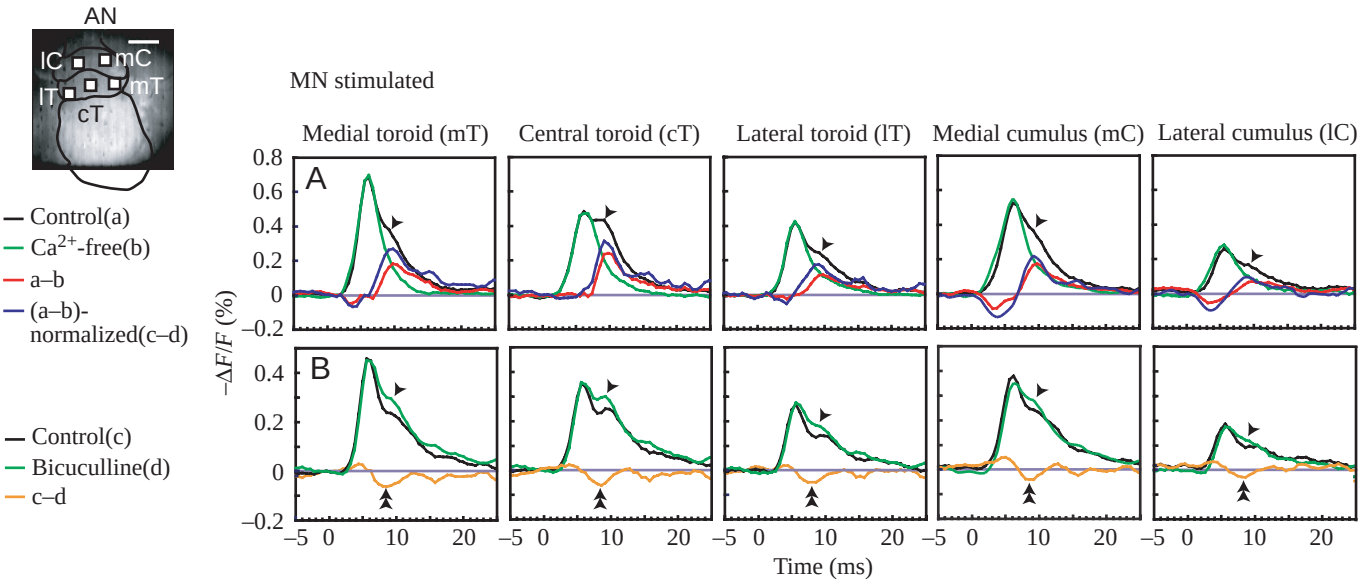

Fig. 6. Time course of the effect of Ca^{2+}-free saline (A) or 10^{-4} mol l^{-1} bicuculline (B) on the optical signals in the antennal lobe (AL) evoked by stimulation of the medial nerve (MN). The optical signals were compared in five square areas (mT, cT, lT, mC and lC). The optical signals were filtered at 246 Hz (=F_c). Scale bar in real image, 100 µm. (A) Slow components (arrowheads) were blocked under Ca^{2+}-free conditions (green lines). Postsynaptic activities (red lines) were calculated by subtracting the response under Ca^{2+}-free saline conditions (green lines) from the response under normal saline conditions (black lines). The excitatory postsynaptic responses (blue lines) were calculated by subtracting each normalized GABAergic optical response from the postsynaptic optical response (red lines). The peak amplitudes of the excitatory postsynaptic responses in the optical signals in the mT, cT and mC were significantly larger than those of the lT and the lC, respectively (see text for details). (B) Bicuculline had no effect on the first peak of the optical signals but increased the second peak of the optical signals (arrowheads on green lines). The possible time course of the GABAergic inhibitory postsynaptic response (orange lines) was calculated by subtracting the responses under bicuculline conditions (green lines) from those under normal conditions (black lines). The maximum amplitudes of the GABAergic inhibitory postsynaptic responses in these MGC sub-regions were not significantly different from each other (double arrowheads).

(1.5±0.5 ms) (P<0.05; paired t-test, N=7; Fig. 9). After washing with normal saline, the time course of the falling phase often recovered to that under normal saline. The amplitudes of the GABAergic inhibitory responses in the MGC sub-regions were not significantly different from each other (all MGC sub-regions in Fig. 6B and in Fig. 8B, P>0.05, one-way repeated-measures ANOVA). These results show that the GABAergic inhibitory responses were equally distributed throughout the MGC sub-regions where an optical response was remarkably evoked.

Excitatory postsynaptic activities

Since polyclonal antibodies raised against GABA have been shown to label all of the AL glomeruli and many somata of AL interneurons in *B. mori* (Yokokawa and Kanzaki, 1997), *M. sexta* (Hoskins et al., 1986) and *P. americana* (Distler, 1990), it has been suggested that GABA is a major transmitter of most inhibitory interneurons in the insect AL. In the present study, excitatory postsynaptic responses were calculated by subtracting GABAergic inhibitory potentials from the postsynaptic activities. Before subtracting, each GABAergic inhibitory potential was calculated using the following equation:

$$\mathrm{nGABA} = A_{\mathrm{Ca\text{-}free}}/A_{\mathrm{bic}} , \quad (1)$$

where nGABA is normalized GABAergic inhibitory potential, $A_{\mathrm{Ca\text{-}free}}$ is the first peak amplitude of optical response under Ca^{2+}-free conditions (green lines in Figs 6A, 8A), and A_{bic} is the first peak amplitude of optical response under bicuculline conditions (green lines in Figs 6B, 8B). This was necessary because in optical recording, the optical responses of the sensory fibers were not of uniform strength at every trial, therefore it was necessary to normalize the optical response by the strength of the optical response of the sensory fibers in each MGC sub-region. The excitatory postsynaptic activities were then calculated using the following equation:

$$PA_{\mathrm{excite}} = PA - \mathrm{nGABA} , \quad (2)$$

where PA_{excite} is the excitatory postsynaptic activities (blue lines in Figs 6A, 8A) and PA is postsynaptic activities (red lines in Figs 6A, 8A).

When the MN was stimulated, the maximum amplitude of the excitatory postsynaptic response of the optical signals in both the mT and cT was significantly larger than that of the lT, and the maximum amplitude of the excitatory postsynaptic response of the optical signals in the mC was also significantly larger than that of the lC (mT>lT, cT>lT, mC>lC, P<0.05; one-way repeated-measures ANOVA; Fig. 7A). When the LN was stimulated, the maximum amplitude of the excitatory

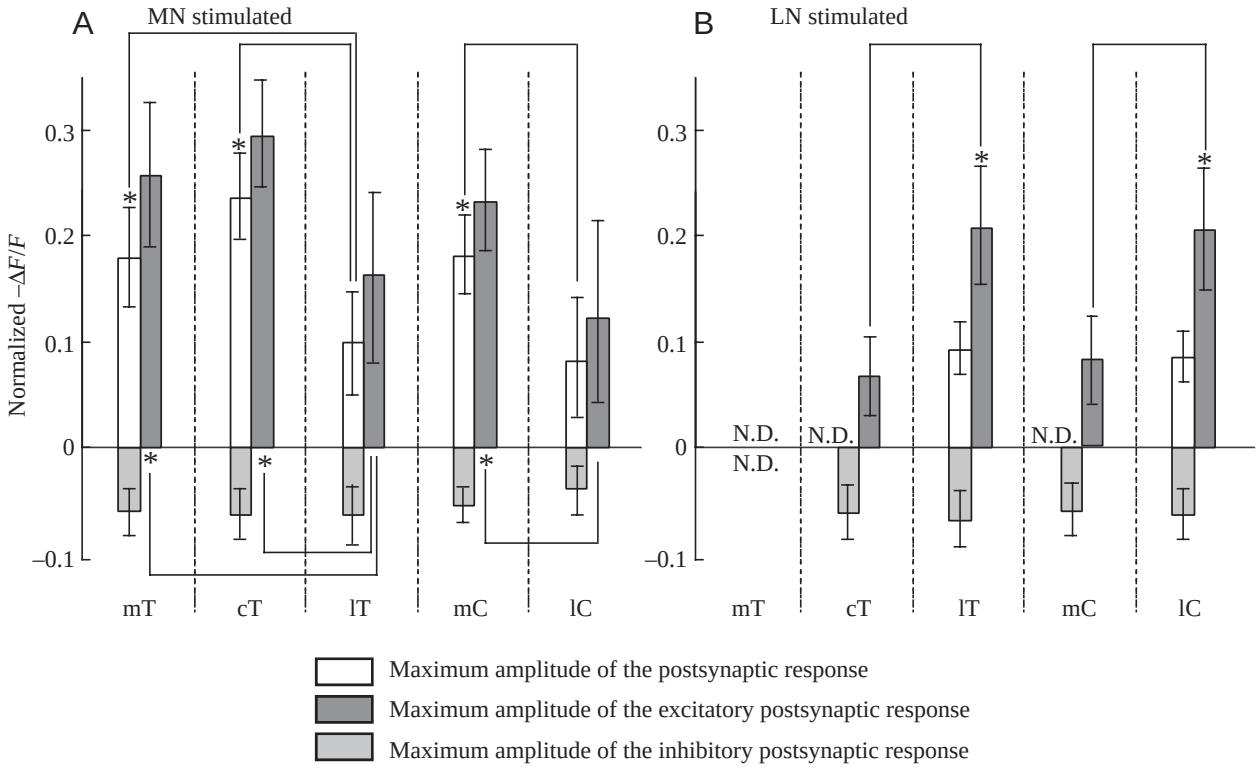

Fig. 7. Comparison of the postsynaptic activity, evoked by stimulation of the medial nerve (MN) and the lateral nerve (LN), among these macroglomerular complex (MGC) sub-regions. The maximum amplitudes of the three responses, the postsynaptic responses, the GABAergic inhibitory postsynaptic responses and the excitatory postsynaptic responses were compared among different MGC sub-regions. (A) When the MN was stimulated, the maximum amplitudes of the postsynaptic responses in the medial toroid (mT) and central toroid (cT) were significantly larger than those of the lateral toroid (lT). In the cumulus, the maximum amplitude of the postsynaptic response in the medial cumulus (mC) was significantly larger than that of the lateral cumulus (lC). Asterisks show that the maximum amplitudes of these responses are significantly different (P<0.05, one-way repeated-measures ANOVA, N=8). The peak amplitudes of the GABAergic inhibitory responses were not significantly different among these MGC sub-regions. (B) When the LN was stimulated, postsynaptic responses in the lT and the lC were detected, but not in other MGC sub-regions. In the toroid, the maximum amplitude of the excitatory postsynaptic response of the lT was significantly larger than that of the cT (P<0.05, one-way repeated-measures ANOVA, N=7). In the cumulus, the maximum amplitude of the postsynaptic response of the lC was significantly larger than that of the mC (P<0.05, one-way repeated-measures ANOVA, N=7). The maximum amplitudes of the GABAergic responses were not significantly different among these MGC sub-regions except mT. N.D., not detected.

postsynaptic response of the optical signal in the lT was significantly larger than that of the cT, and the maximum amplitude of the excitatory postsynaptic response of the optical signals in the lC was also significantly larger than that of the mC (lT>cT and lC>mC, P<0.05; one-way repeated-measures ANOVA; Fig. 7B). These results suggest that the differences in the peak amplitudes of the postsynaptic responses, blocked under Ca^{2+}-free saline conditions (red lines in Figs 6A, 8A), reflect a nonhomologous distribution of excitatory postsynaptic activity (blue lines in Figs 6A, 8A) not of inhibitory postsynaptic activity (orange lines in Figs 6B, 8B).

Discussion

Projection of sensory fibers from the MN and the LN

In *M. sexta*, axons from sensilla on the dorsal surface of the antenna are biased towards the medial part of the MGC and those from ventral sensilla are biased towards the lateral part of the MGC (Christensen et al., 1994). In *B. mori*, fibers from anterior branches (corresponding to the medial nerve) in the antennae are topographically biased towards the medial MGC, while fibers from posterior branches (corresponding to the lateral nerve) are biased towards the lateral MGC, as shown by forward-filling from some sensory hairs (Koontz and Schneider, 1987). We could also demonstrate the difference between the 3-D projection pattern of the MN or the LN by confocal microscopic observation. In the anterior MGC, the projection area of the MN sensory fibers is biased towards the medial MGC, while in the posterior MGC there is no bias in the MGC sub-regions. On the other hand, the projection area of the LN sensory fibers is biased towards the lateral MGC in each depth of the AL. In our optical recording experiments, when the MN was stimulated, the optical response of the sensory fibers was observed throughout the whole MGC even though there is a bias of the optical response in the MGC. By contrast, when the LN was stimulated, the optical response of

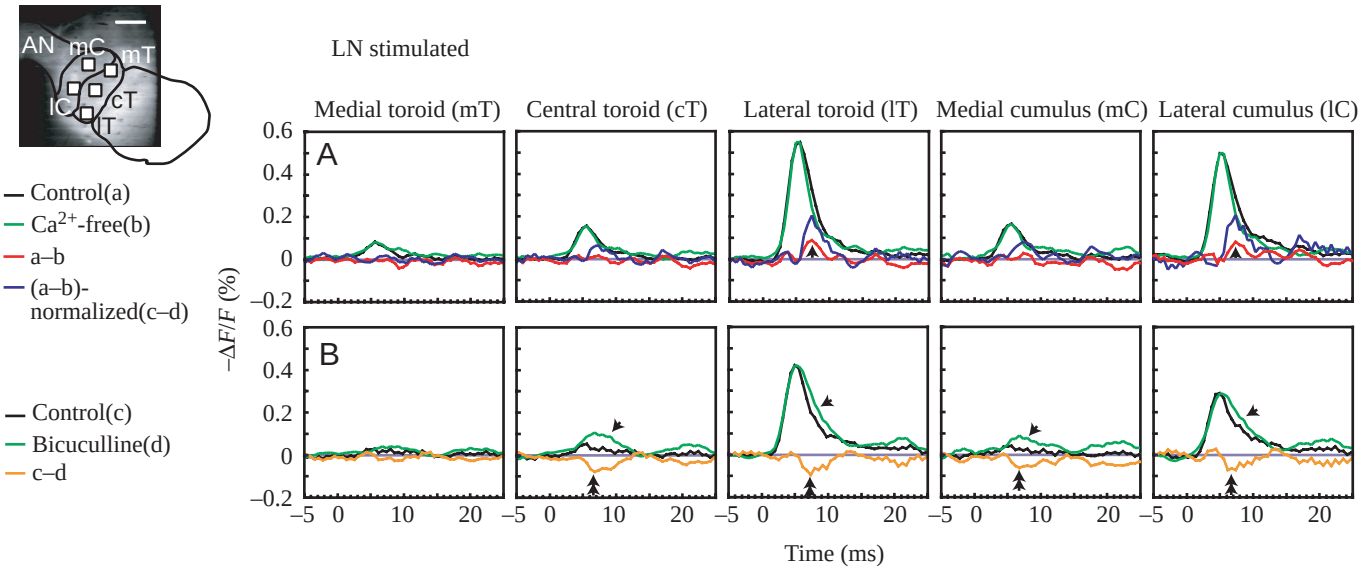

Fig. 8. Time course of the effects of Ca^{2+}-free saline (A) or 10^{-4} mmol l^{-1} bicuculline (B) on the optical signals in the antennal lobe (AL) evoked by stimulation of the lateral nerve (LN). The optical signals were compared in five square areas (mT, cT, lT, mC and lC). The optical signals were filtered at 246 Hz (=F_c). Scale bar in real image, 100 µm. (A) The optical signals under normal saline conditions (black line) were superimposed onto those under Ca^{2+}-free saline conditions (green lines). Postsynaptic activity (red lines), blocked by Ca^{2+}-free saline, was evoked in both the lT and the lC (arrowheads). The peak amplitudes of the excitatory postsynaptic responses (blue lines) in the optical signals in the lT and the lC were significantly larger than those of the other macroglomerular complex (MGC) sub-regions (see text for details). (B) Optical signals blocked by bicuculline were detected in all MGC sub-regions except for the mT (double arrowheads on orange lines). The maximum amplitudes of the GABAergic inhibitory postsynaptic responses in these MGC sub-regions were not significantly different from each other.

the sensory fibers was remarkably observed only in the lateral MGC. These results suggest that the projection pattern of the sensory fibers in the MN is not only segregated in the MGC sub-regions along the medial–lateral axis but also along the anterior–posterior axis through the MGC.

Analysis of the source of the optical response

We succeeded in separating excitatory and inhibitory postsynaptic activities from presynaptic activities in the MGC and demonstrated that MGC sub-regions code not only odor quality but also topological information from the antenna. A model of two opposing parallel pathways in the MGC of *M. sexta* was proposed by Christensen et al. (1998) based on their pharmacological, anatomical and electrophysiological data. These pathways comprise two feedforward pathways and one feedback pathway to the MGC-PNs. One of these feedforward pathways (pathway 1) is a route passing through a GABAergic local interneuron (GABA-LN), resulting in an inhibitory response (I_1) in an MGC-PN. Bicuculline blocks this inhibitory input (I_1). The other feedforward pathway (pathway 2) is a polysynaptic route passing through local interneurons (LNs),

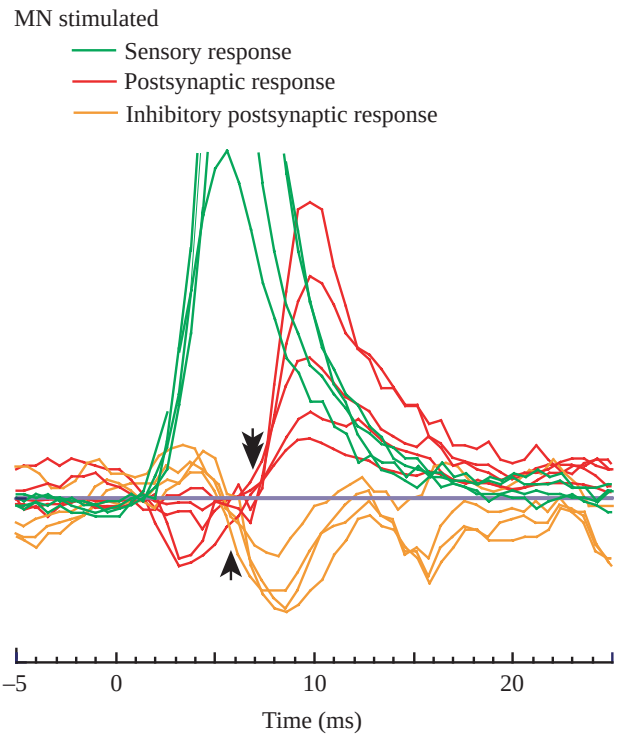

Fig. 9. The GABAergic inhibitory postsynaptic response (arrowhead) always preceded the postsynaptic responses separated under Ca^{2+}-free conditions (double arrowhead). The sensory responses remained under Ca^{2+}-free conditions, postsynaptic responses separated under Ca^{2+}-free conditions and GABAergic inhibitory postsynaptic responses blocked by bicuculline in each MGC sub-region were superimposed. The delay time of the GABAergic inhibitory postsynaptic response from the first peak (0.2±0.2 ms) was shorter than the delay time of the postsynaptic response blocked by Ca^{2+}-free saline (1.5±0.5 ms) (P<0.05; paired t-test, N=7).

resulting in an excitatory response (E) in an MGC-PN. Bicuculline does not block this excitatory pathway. The feedback pathway to MGC-PNs (pathway 3) comprises a feedback neuron (FN) and a GABA-LN, resulting in hyperpolarization (I_2) in the PN. Bicuculline does not block I_2. Recently, in *B. mori*, several types of MGC-PNs were morphologically and physiologically identified (Kanzaki et al., 2003). Kanzaki et al. (2003) showed that there is a difference between the MGC-PN pheromone response patterns of *B. mori* and *M. sexta*. The difference is that, in *M. sexta* MGC-PNs, pheromone stimulation evokes a brief hyperpolarization (I_1) followed by a depolarization with bursting potentials, but in *B. mori* MGC-PNs, I_1 was not observed (Kanzaki et al., 2003). Bicuculline blocks I_1 in *M. sexta* MGC-PNs (Waldrop et al., 1987). In the present study, the postsynaptic activities in the MGC were enhanced under bicuculline conditions. This result suggests that GABAergic inhibitory input also exists in *Bombyx* MGC-PNs, as in *Manduca* MGC-PNs. We do not know the reason why I_1 cannot be observed in *B. mori* MGC-PNs electrophysiologically. With this one exception, there are many similarities between *B. mori* and *M. sexta*, suggesting that there is a similar neural circuit in both MGCs. Assuming that this is the case, we can suppose the following hypothesis about the source of the optical responses.

Pathway 1

In the present study, the inhibitory postsynaptic responses in the MGC were separated under bicuculline conditions (Figs 6B, 8B). Most of the local interneurons in the AL are GABAergic in *M. sexta* (Waldrop et al., 1987; Christensen et al., 1998) and in *P. americana* (Boeckh and Tolbert, 1993; Distler, 1989, 1990). In these studies, most of these LNs have wide field arborizations in the AL. In *B. mori*, wide field LNs were also identified in the AL (Y. Seki, unpublished observations). In the present study, we demonstrated that GABAergic inhibitory responses were uniformly distributed in the whole MGC, where the excitatory postsynaptic activity is generated. It is likely that most of the signals blocked by bicuculline originated from inhibitory postsynaptic potentials of MGC-PNs induced by similar wide field LNs.

Pathways 2 and 3

The inhibitory postsynaptic response always preceded the postsynaptic responses separated under Ca^{2+}-free conditions (Fig. 9). Therefore, we speculate that the excitatory components of the postsynaptic responses separated under Ca^{2+}-free conditions are compound potentials originating from pathways 2 and 3.

Compound excitatory postsynaptic response on pathways 1–3

In the present study, excitatory postsynaptic responses were calculated by subtracting the GABAergic inhibitory responses, blocked by bicuculline, from the postsynaptic responses, blocked by Ca^{2+}-free saline. In the *M. sexta* AL, bicuculline does not block the GABAergic I_2 (Christensen et al., 1998). There is a possibility that the excitatory postsynaptic response includes a GABAergic hyperpolarization (I_2). The GABAergic hyperpolarization (I_2) has a delay time of ~50 ms after I_1 (Christensen et al., 1998). In the present study, the postsynaptic response was separated within a range of <25 ms from the stimulus onset and did not include I_2. This suggests that the excitatory postsynaptic response in the present study is mostly caused by the compound excitatory postsynaptic response of all AL interneurons (pathways 1, 2 and 3).

As shown in Figs 3 and 4, thick fibers pass through the posterior region of the AL. These thick fibers running from the MN pass posteriorly through the central region of the MGC (Fig. 3B,C), and those running from the LN pass posteriorly through the lateral region of the MGC (Fig. 4B,C). Our optical recording focus plane was fixed at 50 μm below the surface of the MGC. However, there is a possibility of recording not only the signal in the MGC but also the signal of these thick fibers because we could not recognize the range in depth to acquire the optical recording. These thick fibers terminate in the AMMC and not in the MGC or the posterior region of the MGC (Koontz and Schneider, 1987). This suggests that postsynaptic responses blocked under Ca^{2+}-free conditions originate purely from the MGC and not from the thick fibers.

Modular organization of the MGC

In the present study, MGC sub-regions, which have high excitatory postsynaptic input from the MN or from the LN, were identified. Our results raise the following question: are there specific interneurons that receive sensory input from topologically specific sensory fibers? In a previous study, it was found that toroid-PNs have distinct tufts in confined regions in the toroid (Kanzaki et al., 2003). Considering these results (Kanzaki et al., 2003) with restricted terminal arborizations of the olfactory receptor neurons (Koontz and Schneider, 1987), it was speculated that specific olfactory receptor neurons contact specific toroid-PNs in confined regions, and such confined regions may play roles as local circuits for olfactory coding (Kanzaki et al., 2003). These results suggest that there is a possibility that the toroid-PNs receive topological information from the MN or the LN and that these parallel pathways send the topological information to higher olfactory centers. By contrast, the cumulus-PNs did not have distinct tufts but had their dendritic arborizations uniformly distributed in several cumulus sub-regions. In the cumulus there is a possibility that some common PNs receive synaptic input from the sensory fibers either in the MN or in the LN. Kanzaki et al. (2003) also demonstrated that (1) toroid-PNs send sparse terminals to restricted areas in the calyces of the mushroom body (MB) and dense, widely branching terminals to the inferior lateral protocerebrum (ILPC) and that (2) cumulus-PNs send dense, widely branching terminals to the MB and small branching terminals to the ILPC. We have not yet determined if this topological information is retained in the ILPC and in the MB. It is our ongoing work to investigate whether projection neurons that have dendritic arborizations restricted to a certain sub-region in the toroid have specific response patterns (or topological response patterns) to the stimulation applied to the

medial or lateral flagella, and whether these PNs have projection areas in certain areas in the ILPC and in the MB.

In the present study, we used multi-site optical recording to reveal functional differences in MGC sub-regions. Our results will contribute to gaining a better understanding of the processing of topological information from the antenna in the insect brain. We are planning to investigate the spatio-temporal patterns evoked by odor stimulation to the antenna.

We wish to thank Drs E. S. Hill and K. Okada for technical support and commenting on an early draft of this manuscript. This research was supported by a grant from Basic Research Activities for Innovative Bioscience (BRAIB).

References

Ai, H. and Inouchi, J. (1996). Spatial and temporal analysis of evoked neural activity in optical recordings from American cockroach antennal lobes. *Neurosci. Lett.* **216**, 77-80.

Ai, H., Okada, K., Hill, E. S. and Kanzaki, R. (1998). Spatio-temporal activities in the antennal lobe analyzed by an optical recording method in the male silkworm moth *Bombyx mori*. *Neurosci. Lett.* **258**, 135-138.

Bacon, J. P. and Altman, J. S. (1977). A silver intensification method for cobalt-filled neurons in wholemount preparations. *Brain Res.* **138**, 359-363.

Boeckh, J. and Tolbert, L. P. (1993). Synaptic organization and development of the antennal lobe in insects. *Microsc. Res. Technique* **24**, 260-280.

Christensen, T. A., Harrow, I. D., Cuzzocrea, C., Randolph, P. W. and Hildebrand, J. G. (1994). Distinct projections of two populations of olfactory receptor axons in the antennal lobe of the sphinx moth *Manduca sexta*. *Chem. Senses* **20**, 313-323.

Christensen, T. A., Waldrop, B. R. and Hildebrand, J. G. (1998). Multitasking in the olfactory system: context-dependent responses to odors reveal dual GABA-regulated coding mechanisms in single olfactory projection neurons. *J. Neurosci.* **18**, 5999-6008.

Distler, P. (1989). Histochemical demonstration of GABA-like immunoreactivity in cobalt labeled neuron individuals in the insect olfactory pathway. *Histochemistry* **91**, 245-249.

Distler, P. (1990). GABA-immunohistochemistry as a label for identifying types of local interneurons and their synaptic contacts in the antennal lobes of the American cockroach. *Histochemistry* **93**, 617-626.

Hansson, B. S., Christensen, T. A. and Hildebrand, J. G. (1991). Functionally distinct subdivisions of the macroglomerular complex in the antennal lobe of the male sphinx moth *Manduca sexta*. *J. Comp. Neurol.* **312**, 264-278.

Heinbockel, T. and Hildebrand, J. G. (1998). Antennal receptive fields of pheromone-responsive projection neurons in the antennal lobes of the male sphinx moth *Manduca sexta*. *J. Comp. Physiol. A* **183**, 121-133.

Homberg, U., Hoskins, S. G. and Hildebrand, J. G. (1995). Distribution of acetylcholinesterase activity in the deutocerebrum of the sphinx moth *Manduca sexta*. *Cell Tissue Res.* **279**, 249-259.

Hoskins, S. G., Homberg, U., Kingan, T. G., Christensen, T. A. and Hildebrand, J. G. (1986). Immunocytochemistry of GABA in the antennal lobes of the sphinx moth *Manduca sexta*. *Cell Tissue Res.* **244**, 243-252.

Hosl, M. (1990). Pheromone-sensitive neurons in the deutocerebrum of *Periplaneta americana*: receptive fields on the antenna. *J. Comp. Physiol. A* **167**, 321-327.

Jastreboff, P. J., Pederson, P. E., Greer, C. A., Stewart, W. B., Kauer, J. S., Benson, T. E. and Shepherd, G. M. (1984). Specific olfactory receptor populations projecting to identified glomeruli in the rat olfactory bulb. *Proc. Natl. Acad. Sci. USA* **81**, 5250-5254.

Kanzaki, R. and Shibuya, T. (1986). Identification of the deutocerebral neurons responding to the sexual pheromone in the male silkworm moth brain. *Zool. Sci.* **3**, 409-418.

Kanzaki, R., Soo, K., Seki, Y. and Wada, S. (2003). Projections to higher olfactory centers from subdivisions of the antennal lobe macroglomerular complex of the male silkmoth. *Chem. Senses* **28**, in press.

Koontz, M. A. and Schneider, D. (1987). Sexual dimorphism in neuronal projections from the antennae of silk moths (*Bombyx mori*, *Antheraea polyphemus*) and the gypsy moth (*Lymantria dispar*). *Cell Tissue Res.* **249**, 39-50.

Okada, K., Kanzaki, R. and Kawachi, K. (1996). High-speed voltage sensitive dye imaging of an *in vivo* insect brain. *Neurosci. Lett.* **209**, 197-200.

Pedersen, P. E., Jastreboff, P. J., Stewart, W. B. and Shepherd, G. M. (1986). Mapping of an olfactory receptor population that projects to a specific region in the rat olfactory bulb. *J. Comp. Neurol.* **250**, 93-108.

Schoenfeld, T. A., Clancy, A. N., Forbes, W. B. and Macrides, F. (1994). The spatial organization of the peripheral olfactory system of the hamster. I. Receptor neuron projections to the main olfactory bulb. *Brain Res. Bull.* **34**, 183-210.

Shepherd, G. M. (1993). Current issues in the molecular biology of olfaction. *Chem. Senses* **18**, 191-198.

Tolbert, L. P. and Hildebrand, J. G. (1981). Organization and synaptic ultrastructure of glomeruli in the antennal lobes of the moth *Manduca sexta*: a study using thin sections and freeze-fracture. *Proc. R. Soc. Lond.* B **213**, 279-301.

Waldrop, B., Christensen, T. A. and Hildebrand, J. G. (1987). GABA-mediated synaptic inhibition of projection neurons in the antennal lobes of the sphinx moth, *Manduca sexta*. *J. Comp. Physiol. A* **161**, 23-32.

Yokokawa, T. and Kanzaki, R. (1997). Inhibitory interneurons involved in generating the characteristic flip-flopping neural activity for instructing female-searching behavior of a male silkworm moth. *Zool. Sci.* **14 Supplement**, 114.